Pseudoscalar top-Higgs coupling: Exploration of CP-odd observables to resolve the sign ambiguity

Nicolas Mileo,[1, *] Ken Kiers,[2, †] Alejandro Szynkman,[1, ‡] Daniel Crane ,[2, §] and Ethan Gegner[2, ¶]

[1]*IFLP, CONICET – Dpto. de Física, Universidad Nacional de La Plata, C.C. 67, 1900 La Plata, Argentina*

[2]*Physics and Engineering Department, Taylor University, 236 West Reade Ave., Upland, IN 46989, USA*

(Dated: February 10, 2016)

Abstract

We present a collection of CP-odd observables for the process $pp \rightarrow t\, (\rightarrow b\ell^+\nu_\ell)\, \bar{t}\, (\rightarrow \bar{b}\ell^-\bar{\nu}_\ell)\, H$ that are linearly dependent on the scalar (κ_t) and pseudoscalar ($\tilde{\kappa}_t$) top-Higgs coupling and hence sensitive to the corresponding relative sign. The proposed observables are based on triple products (TP) structures that we extract from the expression of the differential cross section in terms of the spin vectors of the top and antitop quarks. In order to explore other possibilities, we progressively modify these TPs, firstly, by combining them and then by replacing the spin vectors by the lepton momenta or the t and $\bar{t}$ momenta by their visible parts. We obtain that the most promising observable can disentangle the hypotheses $\kappa_t = 1, \tilde{\kappa}_t = \pm 1$ by more than $\sim 20\sigma$ for 10^5 events that is within the expected order of magnitude of events at the HL-LHC. In the case of observables that do not need the reconstruction of the t and $\bar{t}$ momenta, the power of discrimination is up to $\sim 16\sigma$ for the same ammount of events. We also show that the capability of the most promising observables for separating the CP-mixed hypotheses preveals even when a number of events plausible within the short term LHC is considered.

----

[*] mileo@fisica.unlp.edu.ar

[†] knkiers@taylor.edu

[‡] szynkman@fisica.unlp.edu.ar

[§] dkcrane@mtu.edu

[¶] ethan˙gegner@taylor.edu

I. INTRODUCTION

After the discovery of a new boson H by the ATLAS [1] and CMS [2] collaborations, it has become of crucial importance its characterization, namely the determination of its physical properties with the highest possible precision. Among the features of the new boson that are under investigation, the study of its couplings to the fermions is of great relevance, allowing us to study the nature of H under the discrete symmetry CP and to clarify the extent to which this new particle is consistent to the Higgs boson predicted by the Standard Model (SM) of particle physics. In particular, the test of the Higgs coupling to the heaviest fermion, the top quark, is a priority since on the one hand, it rules the main production mechanism through gluon fusion and contributes to the important decay mode to two photons, and on the other hand, it is involved in the scalar-field naturalness problem giving rise to the leading dependence on the cut-off energy scale in the corrections to the Higgs mass and it may play an important role in the EWSB mechanism.

Given the fact that the main Higgs boson production process, the gluon fusion, is dominated by a top quark loop and that the diphoton and digluon decay channels are also mediated by a top loop, these processes provide constraints on the scalar and pseudoscalar tH couplings, κ_t and $\tilde{\kappa}_t$ [3–6]. However, these constraints assume that there are no other sources contributing to the corresponding effective couplings and, in the case of the diphoton decay channel which also involves a W boson loop, that the coupling of the Higgs boson to the W is standard. In this sense, the constraints derived from measurements of Higgs rates are indirect constraints. In this direction, electric dipole moments (EDM) can also impose stringent indirect constraints on $\tilde{\kappa}_t$ by assuming that there are no new physics (NP) particles contributing to the loops of the relevant diagrams and that the electron-Higgs coupling is that predicted by the SM [3, 7]. In order to probe directly the tH coupling, processes with smaller cross sections need to be taken into account.

In contrast to the τH coupling which can be studied trough the decay $H \to \tau^+ \tau^-$ [8], the tH coupling is tested directly by making use of the production processes since the phase space forbids the Higgs to decay to the pair $t\bar{t}$. The production of the Higgs boson in association with the pair $t\bar{t}$ and the production in association with a single top or antitop are the only two direct ways of probing the tH coupling. The cross section of the single top (antitop) production is smaller and it is given by the interference between a diagram in which the Higgs is radiated from the top (antitop) leg and one with the Higgs emmited from the intermediate virtual W boson. This then implies that the contraints over κ_t and $\tilde{\kappa}_t$ derived from tH and $\bar{t}H$ production are dependent on the asummption made on the coupling of the Higgs to the gauge boson W, κ_W. However, it is important to note that the interference between the above mentioned diagrams present in tH ($\bar{t}H$) production can be exploited in order to determine the relative sign between κ_t and κ_W (see for example [9]). From the point of view of $t\bar{t}H$ production, several observables sensitive to the couplings κ_t and $\tilde{\kappa}_t$ has been proposed. Examples of such observables are the cross section, the invariant mass distributions, the transverse Higgs momentum distribution or the azymuthal-angle separation between t and $\bar{t}$ just to name a few [10]. An approach based on weighted moments and optimal observables has been developed in [11] to discriminate the hypothesis of a CP-even Higgs from that of a CP-mixed state within the context of a e^+e^- as well as a pp collider. All the mentioned observables are CP-even and hence are not sensitive to relative sign between the scalar and pseudoscalar couplings κ_t and $\tilde{\kappa}_t$. Such observables are quadratically dependent on these couplings and then only provide an indirect measure of CP violation. In order to be sensitive to the relative sign between κ_t and $\tilde{\kappa}_t$, CP-odd observables

must be considered.

Since the quark top decays before it can hadronize, its spin information is passed on to the angular distributions of the decay products in such a way that these particles work as spin analyzers being the lepton the most powerful. On the other hand, it has been shown that in $t\bar{t}$ production the top quark and antiquark spins are strongly correlated [12] and this manifests in the double angular distributions of the decay products of the t and $\bar{t}$ systems. These correlations are dependent in turn on the production mechanism and in the case of $t\bar{t}H$ associated production are sensitive to the manner in which the top couples to the Higgs boson. In fact, observables that exploit the differences on the $t\bar{t}$ spin configurations are used in [13] to improve the discrimination of the $t\bar{t}H$ signal from the dominant irreducible background $t\bar{t}b\bar{b}$, in which the Higgs boson is not involved.

In this paper, we define a set of observables linearly dependent on κ_t and $\tilde{\kappa}_t$ and hence sensitive to the relative sign of these couplings. The proposed observables are based on a particular set of triple product structures (TP) that we extract naturally from the expression of the differential cross section, which makes use in turn of the fact that the kinematics of the decay products contain the information on the t and $\bar{t}$ spins and thus is sensitive to the nature of the tH coupling, just as was discussed in the previous paragraph. By using spinor thechniques we simply relate the top quark and antiquark spin vectors and the corresponding final state particle momenta and separate the production process from the decay which allows to identify straightforwardly the contributions linearly sensitive to the couplings. Further, the TPs correlations in these contributions incorporate the t and $\bar{t}$ spin vectors. Starting with these TPs, we not only recover the observables given in [10, 14] but also propose additional possibilities that increase the sensitivity. In order to establish a hierarchy in the sensitivity of the TPs under analysis we investigate three different types of observables by using simulated events: asymmetries, mean values and angular distributions. We note that TP correlations has been used in [15] in the context of top-quark production and decay and in [16] in the framework of anomalous color dipole operators.

The remainder of this paper is organized as follows. In Sec. II we study the theoretical framework for the process $pp \rightarrow t\,(\rightarrow b\ell^+\nu_\ell)\,\bar{t}\,(\rightarrow \bar{b}\ell^-\bar{\nu}_\ell)\,H$ and derive a general expression for the differential cross section from which a first set of TP correlations is extracted. In Sec. III we probe the sensitivity of these TPs to the tH coupling by using various CP-odd observables. Subsequent sections are dedicated to explore another possibilities of CP-odd observables. In particular, observables based on TPs that incorporate the Higgs momentum are discussed in Sec. IV, whereas observables obtained without using the t and $\bar{t}$ momenta are studied in Sec. V. Finally, Sec. VI is devoted to the discussion on the experimental feasibility of the most promising observables encountered here. The main conclusions are summarized in Sec. VII.

II. PROCESS $pp \rightarrow t(\rightarrow b\ell^+\nu_\ell)\,\bar{t}(\rightarrow \bar{b}\ell^-\bar{\nu}_\ell)\,H$. THEORETICAL FRAMEWORK

At the LHC the $t\bar{t}H$ production proceeds via $q\bar{q}$ annihilation and gg fusion processes. The relevant Feynman diagrams at leading order are displayed in Fig. 1, where the two first rows correspond respectively to $q\bar{q}$ and gg s-channels whereas the last one depicts the gg t-channels. By exchanging the gluon lines in this row, three more gg-initiated diagrams can be obtained. We describe the tH cupling with the effective lagrangian

$$\mathcal{L}_{t\bar{t}H} = -\frac{m_t}{v}(\kappa_t\bar{t}t + i\tilde{\kappa}_t\bar{t}\gamma_5 t)H, \tag{1}$$

where $v = 246$ GeV is the SM Higgs vacuum expectation value, and the coefficients κ_t and $\tilde{\kappa}_t$ determine the weigth of the scalar and pseudoscalar interaction, respectively. The SM case is obtained for $\kappa_t = 1$ and $\tilde{\kappa}_t = 0$, while the values $\kappa_t = 0$ and $\tilde{\kappa}_t \neq 0$ parameterizes a CP-odd Higgs.
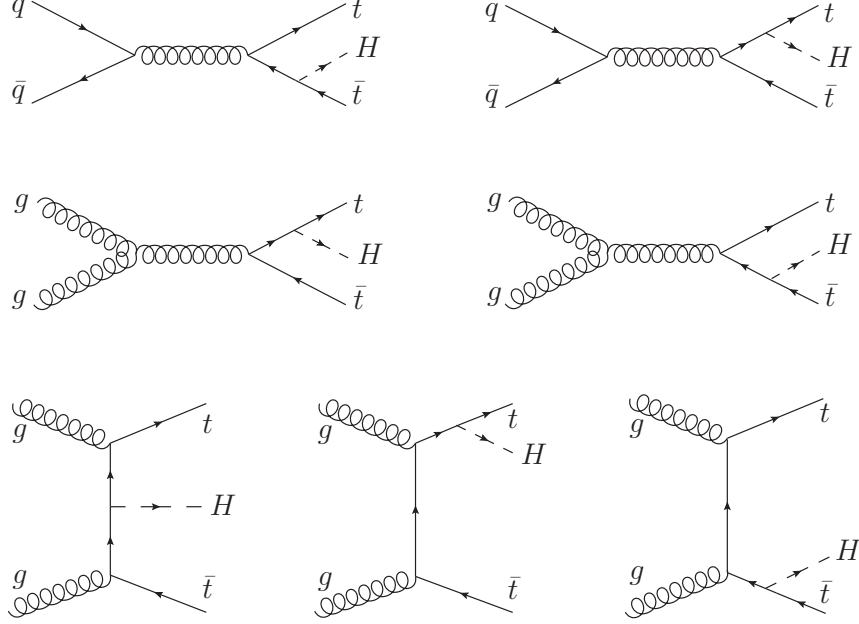

FIG. 1: Tree level Feynman diagrams contributing to $t\bar{t}H$ production at the LHC. Three more diagrams are obtained by exchanging the gluon lines in the t-channel diagrams.

Since the total cross-section is dominated by the gg contribution, let us focus on the gg-initiated production followed by the leptonic SM decay of both t and $\bar{t}$. By using the narrow-width approximation for the top quark, it can be shown that the unpolarized differential cross section for the full process $gg \to t(\to b\ell^+\nu_\ell)\,\bar{t}(\to \bar{b}\ell^-\bar{\nu}_\ell)\,H$ takes the following form (we sketch the proof below)

$$d\sigma = \sum_{\substack{b\ell^+\nu_l \\ \text{spins}}} \sum_{\substack{\bar{b}\ell^-\bar{\nu}_\ell \\ \text{spins}}} \left(\frac{2}{\Gamma_t}\right)^2 d\sigma(gg \to t(n_t)\bar{t}(n_{\bar{t}})H)\, d\Gamma(t(n_t) \to b\ell^+\nu_\ell)\, d\Gamma(\bar{t}(n_{\bar{t}}) \to \bar{b}\ell^-\bar{\nu}_\ell), \quad (2)$$

where $d\sigma(gg \to t(n_t)\bar{t}(n_{\bar{t}})H)$ is the differential cross section of the production of a top quark with spin vector n_t plus an anti-top quark with spin vector $n_{\bar{t}}$ and a Higgs boson, whereas $d\Gamma(t(n_t) \to b\ell^+\nu_\ell)$ and $d\Gamma(\bar{t}(n_{\bar{t}}) \to \bar{b}\ell^-\bar{\nu}_\ell)$ are the differential decay widths of a top with spin vector n_t and an anti-top with spin vector $n_{\bar{t}}$, respectively. Also, the vectors n_t and $n_{\bar{t}}$ are given

by particular combinations of the momenta t, ℓ^+ and $\bar{t}, \ell^-$ respectively [17],

$$n_t = -\frac{p_t}{m_t} + \frac{m_t}{(p_t \cdot p_{\ell^+})} p_{\ell^+} \tag{3}$$

$$n_{\bar{t}} = \frac{p_{\bar{t}}}{m_t} - \frac{m_t}{(p_{\bar{t}} \cdot p_{\ell^-})} p_{\ell^-}. \tag{4}$$

Expressions similar to Eq. (2) have been derived for the production of short-lived particles in e^-e^+ colliders [18] and in particular for $t\bar{t}$ production both in e^-e^+ colliders [17] and pp colliders [19].

We will outline now how to derive Eq. (2) and to obtain the above definitions for the spin vectors. The process $g_a g_b \to t(\to b_i \ell^+ \nu_\ell) \bar{t}(\to \bar{b}_j \ell^- \bar{\nu}_\ell) H$ can be drawn as in Fig. 2, where a and b denote the gluons and i and j are the top and anti-top colours.
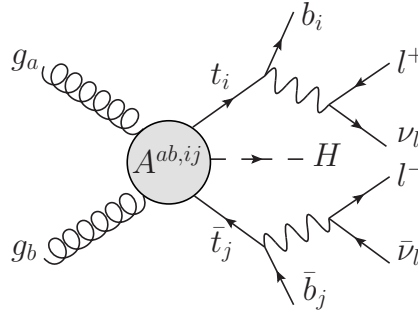

FIG. 2: Schematic representation of the process $g_a g_b \to t(\to b_i \ell^+ \nu_\ell) \bar{t}(\to \bar{b}_j \ell^- \bar{\nu}_\ell) H$. The indices i, j denote the colour of the quarks while a, b are gluon indices.

The diagrams displayed in Fig. 1 (second and third rows) contribute to the quantity $A^{ab,ij}$, so that

$$\mathcal{A}^{ab,ij} \equiv A^{ab,ij}_{\mu\nu}(\epsilon_{\lambda_a})^\mu (\epsilon_{\lambda_b})^\nu = \sum_{k=1}^{8} \mathcal{A}^{ab,ij}_k = \kappa_t \sum_{k=1}^{8} \mathcal{S}^{ab,ij}_k + i\tilde{\kappa}_t \sum_{k=1}^{8} \mathcal{P}^{ab,ij}_k, \tag{5}$$

where ϵ_{λ_a} and ϵ_{λ_b} are the polarization vectors of g_a and g_b respectively and in the last equality the scalar piece of each diagram has been separated from the pseudoscalar one. The quantity $\mathcal{A}^{ab,ij}$ can be linked to the final states particles by using two spinors, ψ_t and $\psi_{\bar{t}}$, that will contain the information on the decay of the virtual top and anti-top, respectively. Hence, the amplitude for the complete process depicted in Fig. 2 can be witten as

$$\mathcal{M}^{ab,ij} = \bar{\psi}_t \, \mathcal{A}^{ab,ij} \, \psi_{\bar{t}}. \tag{6}$$

If we assume b, l and ν_l to be massless, we can make use of the spinor techniques[1] developed in

_____

[1] These spinors techniques can also be used for massive particles. However, the derivation of Eq. (2) is much simpler by assuming the final state particles to be massless which is a sensible approximation in view of the energy involved in the process.

[20] to write $\bar{\psi}_t$ and $\psi_{\bar{t}}$ as follows

$$\bar{\psi}_t = -g^2 \frac{1}{(t^2 - m_t^2 + im_t\Gamma_t)} \frac{1}{((t-b)^2 - M_W^2 + im_W\Gamma_W)} \langle b - |\nu_\ell+\rangle\langle\ell^+ + |(\slashed{\ell} + m_t) \qquad (7)$$

$$\psi_{\bar{t}} = -g^2 \frac{1}{(\bar{t}^2 - m_t^2 + im_t\Gamma_t)} \frac{1}{((\bar{t}-\bar{b})^2 - M_W^2 + im_W\Gamma_W)} \langle\bar{\nu}_\ell + |\bar{b}-\rangle(\slashed{\bar{\ell}} - m_t)|\ell^- +\rangle, \qquad (8)$$

where $|i + (-)\rangle \equiv P_{R(L)}\,\psi_i$ ($P_{R,L} = (1 \pm \gamma^5)/2$) represents a right-handed(left-handed) chiral spinor for particle i, $\langle i + (-)|$ is the corresponding adjoint spinor and we have denoted the momenta through the symbols that represents the name of the particles [21]. The relevant quantity is $|\mathcal{M}^{ab,ij}|^2$, which from Eqs. (6)-(8) is proportional to $((t^2 - m_t^2)^2 + m_t^2\Gamma_t^2)^{-1}$ and $((\bar{t}^2 - m_t^2)^2 + m_t^2\Gamma_t^2)^{-1}$. Under the narrow-width approximation we can replace these factors by $(\pi/m_t\Gamma_t)\delta(t^2 - m_t^2)$ and $(\pi/m_t\Gamma_t)\delta(\bar{t}^2 - m_t^2)$ respectively. Hence, we can take directly $t^2 = \bar{t}^2 = m_t^2$ in the amplitude and write

$$\mathcal{M}^{ab,ij} = -g^4\,\mathbb{P}_t(t)\,\mathbb{P}_{\bar{t}}(\bar{t})\,\mathbb{P}_W(t-b)\,\mathbb{P}_W(\bar{t}-\bar{b})\,\langle b - |\nu_\ell+\rangle\langle\bar{\nu}_\ell + |\bar{b}-\rangle\sqrt{2(t\cdot\ell^+)}\sqrt{2(\bar{t}\cdot\ell^-)}\,[\bar{\phi}_t\mathcal{A}^{ab,ij}\phi_{\bar{t}}],$$
$$(9)$$

where we have used the notation $\mathbb{P}_t(t) = (t^2 - m_t^2 + im_t\Gamma_t)^{-1}$, $\mathbb{P}_{\bar{t}}(\bar{t}) = (\bar{t}^2 - m_t^2 + im_t\Gamma_t)^{-1}$, $\mathbb{P}_W(t-b) = ((t-b)^2 - M_W^2 + im_W\Gamma_W)^{-1}$ and $\mathbb{P}_W(\bar{t}-\bar{b}) = ((\bar{t}-\bar{b})^2 - M_W^2 + im_W\Gamma_W)^{-1}$. The spinors ϕ_t and $\phi_{\bar{t}}$ are defined as follows

$$\phi_t = \frac{(\slashed{\ell} + m_t)}{\sqrt{2(t\cdot\ell^+)}}|\ell^+ +\rangle \qquad (10)$$

$$\phi_{\bar{t}} = \frac{(\slashed{\bar{\ell}} - m_t)}{\sqrt{2(\bar{t}\cdot\ell^-)}}|\ell^- +\rangle \qquad (11)$$

and describe a top quark with spin vector n_t and an anti-top quark with spin vector $n_{\bar{t}}$, since the corresponding projection operators are given by

$$\phi_t\,\bar{\phi}_t = \frac{1}{2}(1 + \slashed{n}_t\gamma^5)(\slashed{\ell} + m_t) \qquad (12)$$

$$\phi_{\bar{t}}\,\bar{\phi}_{\bar{t}} = \frac{1}{2}(1 + \slashed{n}_{\bar{t}}\gamma^5)(\slashed{\bar{\ell}} - m_t), \qquad (13)$$

with n_t and $n_{\bar{t}}$ being the vectors defined in Eq. (3)-(4). Moreover, if we use these spinors to compute the amplitude for a top(anti-) with spin vector $n_t(n_{\bar{t}})$ to decay into $b\ell^+\nu_\ell(\bar{b}\ell^-\bar{\nu}_\ell)$ we obtain

$$\mathcal{M}(t(n_t) \to b\ell^+\nu_\ell) = ig^2\mathbb{P}_W(t-b)\langle b - |\nu_\ell+\rangle\sqrt{2(t\cdot\ell^+)} \qquad (14)$$

$$\mathcal{M}(\bar{t}(n_{\bar{t}}) \to \bar{b}\ell^-\bar{\nu}_\ell) = ig^2\mathbb{P}_W(\bar{t}-\bar{b})\langle\bar{\nu}_\ell + |\bar{b}-\rangle\sqrt{2(\bar{t}\cdot\ell^-)}. \qquad (15)$$

On the other hand, the term inside the square brackets in Eq. (9) is nothing but the amplitude for producing a top quark with spin vector n_t, along with an anti-top with spin vector $n_{\bar{t}}$ and a Higgs boson, i.e.

$$\mathcal{M}(g_a g_b \to t^i(n_t)\bar{t}^j(n_{\bar{t}})H) = \bar{\phi}_t\mathcal{A}^{ab,ij}\phi_{\bar{t}}. \qquad (16)$$

6

By combining Eqs. (14)-(16), we can write Eq. (9) as follows

$$\mathcal{M}^{ab,ij} = \mathbb{P}_t(t)\mathbb{P}_{\bar{t}}(\bar{t})\,\mathcal{M}(t(n_t) \to b\ell^+\nu_\ell)\,\mathcal{M}(\bar{t}(n_{\bar{t}}) \to \bar{b}\ell^-\bar{\nu}_\ell)\,\mathcal{M}(g_a g_b \to t^i(n_t)\bar{t}^j(n_{\bar{t}})H). \quad (17)$$

From Eq. (17), Eq. (2) can be derived. It's important to note that, even though Eqs. (2) and (9) appear to be factorized into production and decay parts, these are not independent, since both parts share kinematical variables due to the presence of the spin vectors n_t and $n_{\bar{t}}$ (see Eqs. (14)-(16) along with the definitions given in Eqs. (3) and (4)).

Let us focus now in the production amplitude in Eq. (17) needed for computing the production part of the unpolarized differential cross-section. By summing over colour and gluon indices we have

$$\sum_{\substack{a,b \\ i,j}} |\mathcal{M}(g_a g_b \to t^i(n_t)\bar{t}^j(n_{\bar{t}})H)|^2 = \sum_{\substack{a,b \\ i,j}} \left| \sum_{k=1}^{8} C_k^{ab,ij}\,\bar{\phi}_t(\kappa_t \mathcal{S}_k + i\tilde{\kappa}_t \mathcal{P}_k)\phi_{\bar{t}} \right|^2, \quad (18)$$

where we have separated the colour structure of each diagram by using the definitions $\mathcal{S}^{ab,ij} = C_k^{ab,ij}\mathcal{S}$ and $\mathcal{P}^{ab,ij} = C_k^{ab,ij}\mathcal{P}$. Also, the factors $g_s^2 m_t/v$ and $-ig_s^2 m_t/v$ arising from the vertices of the t- and s-channel diagrams respectively have been included in the definition of $C_k^{ab,ij}$ for convenience. The terms linear in κ_t and $\tilde{\kappa}_t$ can be written as

$$\mathcal{O}(\kappa_t\tilde{\kappa}_t) \to \frac{1}{2}\kappa_t\tilde{\kappa}_t \sum_{k,r} \mathbb{C}_{kr}\mathrm{Im}\left\{ \mathrm{Tr}\left[(1 + \slashed{n}_t\gamma^5)(\slashed{t} + m_t)\mathcal{S}_k(1 + \slashed{n}_{\bar{t}}\gamma^5)(\slashed{\bar{t}} - m_t)\tilde{\mathcal{P}}_r \right] \right\}, \quad (19)$$

where the factor $\mathbb{C}_{kr} = \sum_{ab,ij} C_k^{ab,ij}C_r^{ab,ij*}$ is real and $\tilde{\mathcal{P}}_r = \gamma^0\mathcal{P}_r\gamma^0$. The only contributing terms are those with an odd number of γ^5 matrices and will lead to triple-products (TP) structures, i.e. contractions between the levi-civita tensor $\epsilon_{\alpha\beta\gamma\delta}$ with four momenta. In contrast, it can be seen from Eq. (18) that the terms proportional to κ_t^2 and $\tilde{\kappa}_t^2$ contain an even number of γ^5 matrices and can be written in terms of scalar products of the available momenta.

In order to state this more clearly, we will consider the form of the differential cross-section in terms of the momenta $q = (q_1 - q_2)/2$, $Q = (q_1 + q_2)/2$, t, $\bar{t}$, n_t and $n_{\bar{t}}$, where $q_{1,2}$ denote the momenta of the gluons. Note that with this choice, $q \cdot Q = 0$ and $Q^2 = -q^2 = M_{t\bar{t}H}^2/4$, where $M_{t\bar{t}H}$ is the invariant mass of the system $t\bar{t}H$. From these six vectors, fifteen TPs can be built[2], and the general form of the production differential cross-section will be given by

$$d\sigma(gg \to t(n_t)\bar{t}(n_{\bar{t}})H) = \kappa_t^2\,f_1(p_i \cdot p_j) + \tilde{\kappa}_t^2\,f_2(p_i \cdot p_j) + \kappa_t\tilde{\kappa}_t \sum_{l=1}^{15} g_l(p_i \cdot p_j)\,\epsilon_l, \quad (20)$$

where $\epsilon_l = \epsilon_{\alpha\beta\gamma\delta}\,p_a^\alpha p_b^\beta p_c^\gamma p_d^\delta$ denotes the lth TP, the Roman indices refer to any of the involved momenta and we adopt the convention $\epsilon_{0123} = +1$. The functions $f_{1,2}$ and g_k depend only on the possible scalar products and are therefore even under a parity transformation (P). However, the terms linear in $\kappa_t\tilde{\kappa}_t$ are P-odd due to the presence of the P-odd TPs. Hence, only the functions $f_{1,2}$ will contribute to the total cross-section, whereas the TPs terms will be sensitive to the sign of the anomalous coupling $\tilde{\kappa}_t$. From the fifteen TPs mentioned above, we will focus on those that do not include q and contain both spin vectors n_t and $n_{\bar{t}}$. The former

---

[2] We note that these fifteen TPs are not linearly independent (see the epsilon relations discussed in [22]).

is motivated in the fact that q cannot be eliminated in terms of the momenta of final state particles (like Q in virtue of momentum-energy conservation). The latter takes into account that for $t\bar{t}$ production at hadron colliders the top and antitop are not polarized but their spins are strongly correlated and observables combining the decay products of t and $\bar{t}$ will be sensitive to this spin correlation [23]. A similar behaviour is expected in $t\bar{t}H$ production where it can be shown that the single-spin asymmetries vanish [13, 14]. Hence, in order to construct observables sensitive to the structure of the tH coupling, we will prefer those TPs that include information on the decay products of both top and anti-top quarks. Only five of the fifteen TPs in Eq. (20) do not involve the vector q and, among these, we will focus on the three that include both n_t and $n_{\bar{t}}$:

$$\epsilon_1 \equiv \epsilon(t, \bar{t}, n_t, n_{\bar{t}}), \tag{21}$$

$$\epsilon_2 \equiv \epsilon(Q, \bar{t}, n_t, n_{\bar{t}}), \tag{22}$$

$$\epsilon_3 \equiv \epsilon(Q, t, n_t, n_{\bar{t}}). \tag{23}$$

Finally, we remark that even though all the above discussion was given within the context of gg-initiated production, similar conclusions are obtained for $q\bar{q}$-initiated production. In particular, the definitions of the spin vectors in Eqs. (3)-(4) and the general form of $d\sigma$ introduced in Eq. (20) are valid in both cases.

III.   CP-ODD OBSERVABLES

We present below three types of observables based on the TPs discussed in Sec. II, mean values, asymmetries and angular distributions. These observables are sensitive not only to the magnitude of the pseudoscalar coupling $\tilde{\kappa}_t$ but also to its sign. With the aim of testing them, we have used in all the cases a set of 10^5 events $pp \to t\,(\to b\ell^+\nu_\ell)\,\bar{t}\,(\to \bar{b}\ell^-\bar{\nu}_\ell)\,H$ simulated at parton level with `MadGraph5_aMC@NLO` [24] at a center-of-mass energy of $14\,\mathrm{TeV}$ for different values of the couplings κ_t and $\tilde{\kappa}_t{}^3$. We have used this somewhat large number of events with the aim of determining clearly the extent to which the proposed observables are sensitive to the NP coupling. However, we will discuss the corresponding experimental viability in Sec. VI. Finally, we have also imposed the following set of cuts: p_T of leptons $> 10\,\mathrm{GeV}$, $|\eta|$ of leptons < 2.5, $|\eta|$ of b jets < 2.5 and $\Delta R_{\ell\ell} > 0.4$.

Under the assumption of no other new physics sources but the inclusion of the pseudoscalar coupling $\tilde{\kappa}_t$, indirect contraints based on the Higgs production from gluon fusion followed by its decay to two photons disfavour $\kappa_t < 0$ without resolving the degeneracy in the sign of $\tilde{\kappa}_t$ [10]. On the other hand, by assuming the tensor structure of the Lagrangian to be the same as in the SM and considering a parameterization with one universal Higgs coupling to vector bosons, κ_V, and one universal Higgs coupling to fermions, κ_f, the measured signal strengths provided by ATLAS and CMS collaborations are compatible with the values predicted by the SM, $(\kappa_f = 1, \kappa_V = 1)$. Based on these facts, we will set the value of the scalar coupling to its SM value, $\kappa_t = 1$, and concentrate in modifications of the value as well as the sign of the pseudoscalar coupling. In particular, we have analized the cases $\tilde{\kappa}_t = 0, \pm 0.25, \pm 0.5, \pm 0.75, \pm 1$. However, we will give some results and comments regarding the pure CP-odd hypothesis $(\kappa_t = 0, \tilde{\kappa}_t = 1)$.

---

[3] Although we use the same number of events in all the cases, the required luminosities are different since the cross section depends on the value of $\tilde{\kappa}_t$.

A. Asymmetry

The first type of CP-odd observable we will consider is the asymmetry. For a certain TP, we define an asymmetry which gives the balance between the number of events with $\epsilon > 0$ and those for which $\epsilon < 0$:

$$\mathcal{A}(\epsilon) = \frac{N(\epsilon > 0) - N(\epsilon < 0)}{N(\epsilon > 0) + N(\epsilon < 0)}. \tag{24}$$

Based on the general expression given in Eq. (20), we expect the following shape for the asymmetry,

$$\mathcal{A}(\epsilon) = \frac{A\kappa_t\tilde{\kappa}_t}{B\kappa_t^2 + C\tilde{\kappa}_t^2}, \tag{25}$$

which for $\kappa_t = 1$ can be parameterized as

$$\mathcal{A}(\epsilon) = \frac{a\tilde{\kappa}_t}{1 + b\tilde{\kappa}_t^2}, \tag{26}$$

where the parameter $a \equiv A/B$ determines the sensitivity to the pseudoscalar coupling, whereas $b \equiv C/B$ quantifies the deviation from the linear behaviour. The results for $\kappa_t = 1$ and $\tilde{\kappa}_t = 0, \pm 1$ are shown in Table I, where the values in terms of the corresponding statistical uncertainty are also included. It can be seen that the considered asymmetries are useful to separate the CP-mixed cases from the SM case and also to discriminate the different sign of $\tilde{\kappa}_t$, giving deviations of order 10σ in the former case and 20σ in the latter.

The sensitivity of the asymmetry is quite similar for the three TPs, as can be seen by including other values of $\tilde{\kappa}_t$ and using the expression in Eq. (26) as fitting function (see Fig. 3). In fact, we obtain the fit parameters $(a = -0.057 \pm 0.006, b = 0.5 \pm 0.2)$, $(a = -0.056 \pm 0.006, b = 0.5 \pm 0.2)$ and $(a = 0.058 \pm 0.006, b = 0.6 \pm 0.2)$ for ϵ_1, ϵ_2 and ϵ_3, respectively. In addition, we include in Fig. 4 the asymmetry for ϵ_1 isolating the gg-initiated, $q\bar{q}$-initiated and pp production. We see that the asymmetry is enhanced for gg-initiated production, while it is reduced and of opposite sign for the $q\bar{q}$-initiated case. The asymmetry for the pp case is then dominated by the gg contribution, albeit smaller due to the $q\bar{q}$ contribution.

TABLE I: Asymmetries obtained by using 10^5 simulated events for the TPs $\epsilon_1 = \epsilon(t, \bar{t}, n_t, n_{\bar{t}})$, $\epsilon_2 = \epsilon(Q, \bar{t}, n_t, n_{\bar{t}})$ and $\epsilon_3 = \epsilon(Q, t, n_t, n_{\bar{t}})$ in the SM case and the two CP-mixed cases defined by $\kappa_t = 1, \tilde{\kappa}_t = \pm 1$.

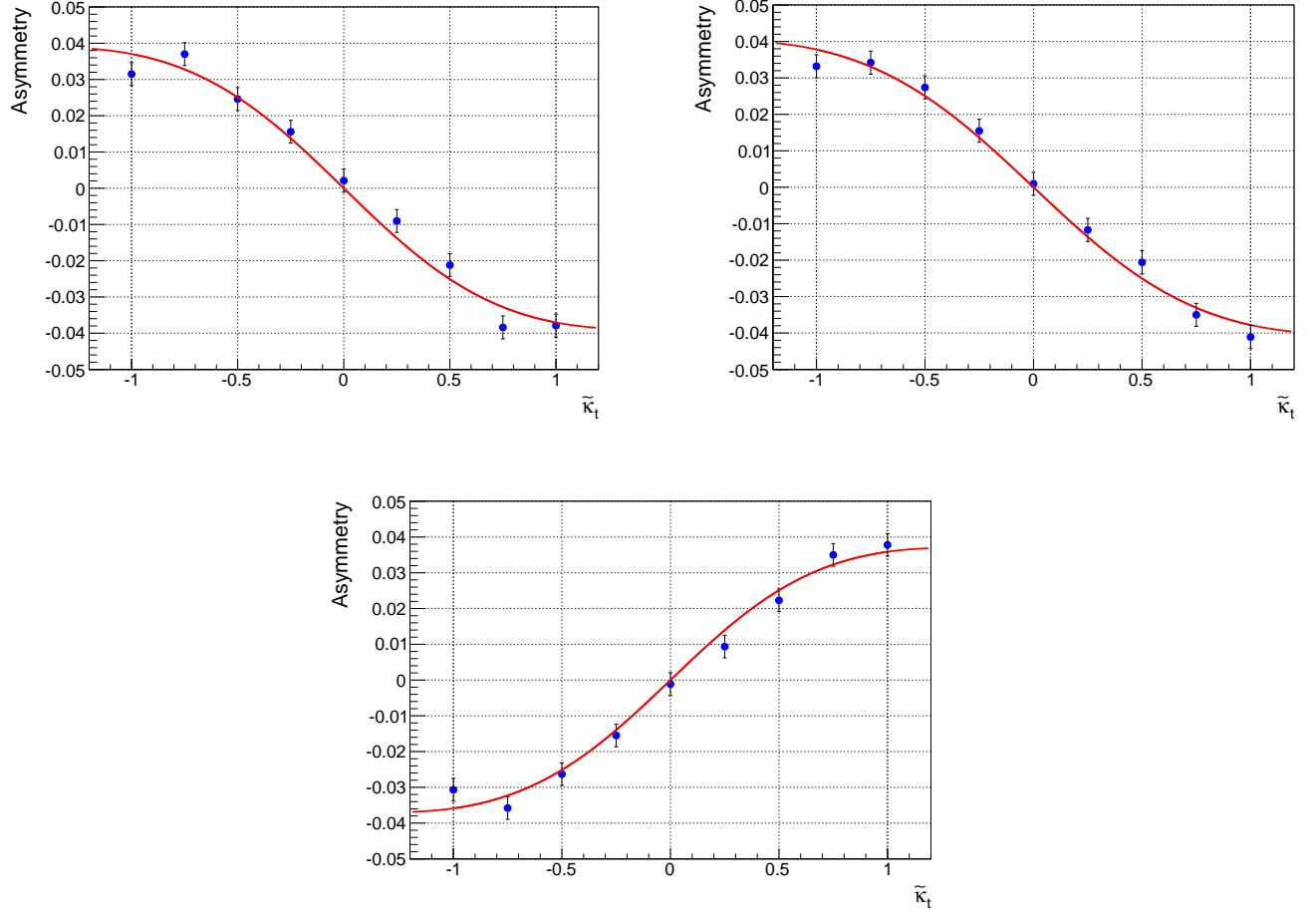| κ_t	$\tilde{\kappa}_t$	$\mathcal{A}(\epsilon_1)$	$\mathcal{A}(\epsilon_1)/\sigma_{\mathcal{A}}$	$\mathcal{A}(\epsilon_2)$	$\mathcal{A}(\epsilon_2)/\sigma_{\mathcal{A}}$	$\mathcal{A}(\epsilon_3)$	$\mathcal{A}(\epsilon_3)/\sigma_{\mathcal{A}}$
1	-1	0.0315	10.0	0.0332	10.5	-0.0307	-9.7
1	0	-0.0021	-0.7	0.0009	0.3	-0.0011	-0.3
1	1	-0.0379	-12.0	-0.0411	-13.0	0.0378	12.0

FIG. 3: Asymmetries for the TPs $\epsilon_1 = \epsilon(t, \bar{t}, n_t, n_{\bar{t}})$ (top-left), $\epsilon_2 = \epsilon(Q, \bar{t}, n_t, n_{\bar{t}})$ (top-right) and $\epsilon_3 = \epsilon(Q, t, n_t, n_{\bar{t}})$ (bottom). The points represent the values for $\tilde{\kappa}_t = 0, \pm 0.25, \pm 0.5, \pm 0.75, \pm 1$ and the red solid line is the fitting curve.
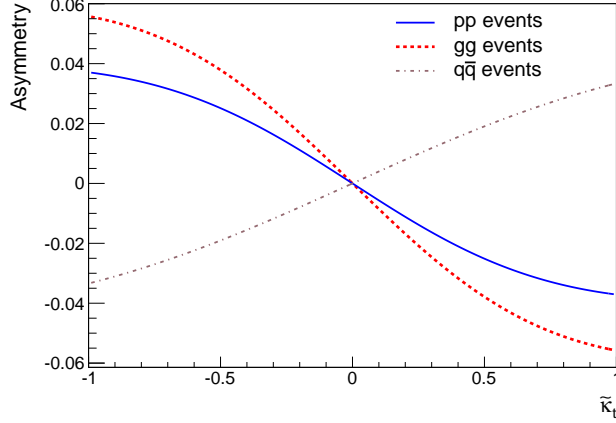
FIG. 4: Asymmetry for the TP $\epsilon_1 = \epsilon(t, \bar{t}, n_t, n_{\bar{t}})$. The dashed line (red) corresponds to gg-initiated production, the dot-dashed line (grey) to $q\bar{q}$-initiated production and the solid line (blue) to pp production.

On the other hand, we have also tested various linear combinations of the TPs $\epsilon_{1,2,3}$, with the result that the asymmetry is enhanced in the following case:

$$\epsilon_4 = \epsilon_3 - \epsilon_2 = \epsilon(Q, t - \bar{t}, n_t, n_{\bar{t}}). \tag{27}$$

Note that in the Q rest frame $\epsilon_4 = Q^0(\vec{t} - \vec{\bar{t}}) \cdot (\vec{n}_t \times \vec{n}_{\bar{t}})$ and the sign of this TP is determined by the quantity $(\vec{t} - \vec{\bar{t}}) \cdot (\vec{n}_t \times \vec{n}_{\bar{t}})$. The values obtained for the asymmetry of this TP are shown in II. We see by comparing the results in Tables I and II that the capability of the asymmetry to separate the two CP-mixed hypotheses is increased by at least 3σ.

TABLE II: Asymmetry for the TP ϵ_4 for the SM case and the two CP-mixed cases defined by $\kappa_t = 1, \tilde{\kappa}_t = \pm 1$. The values are obtained by using 10^5 simulated events.

κ_t	$\tilde{\kappa}_t$	$\mathcal{A}(\epsilon_4)$	$\mathcal{A}(\epsilon_4)/\sigma_{\mathcal{A}}$
1	-1	-0.0371	-12
1	0	0.0004	0.1
1	1	0.0461	14

Finally, it is worth noting that the asymmetry is not useful for discriminating between the SM hypothesis ($\kappa_t = 1, \tilde{\kappa}_t = 0$) and the pure pseudoscalar hypothesis ($\kappa_t = 0, \tilde{\kappa}_t = 1$) because, being linear in both κ_t and $\tilde{\kappa}_t$, it is expected to vanish in these cases. However, we will show in the next section that there exist angular distributions derived from the TPs that are actually suitable to distinguish these two hyphothesis.

11

B. Angular Distributions

Given a certain TP, it is possible to define asocciated angular distributions that are also sensitive to the pseudoscalar coupling $\tilde{\kappa}_t$. In order to clarify this, let us first consider the TP $\epsilon(t, \bar{t}, n_t, n_{\bar{t}})$. This TP can be written as $\epsilon(t + \bar{t}, \bar{t}, n_t, n_{\bar{t}})$ so that in the reference frame defined by $\vec{t} + \vec{\bar{t}} = 0$ and $\vec{\bar{t}} \parallel \hat{z}$ we have

$$\epsilon(t + \bar{t}, \bar{t}, n_t, n_{\bar{t}}) = M_{t\bar{t}} |\vec{\bar{t}}| (\vec{n}_t \times \vec{n}_{\bar{t}})_z = M_{t\bar{t}} |\vec{\bar{t}}||\vec{n}_t||\vec{n}_{\bar{t}}| \sin\theta_{n_t} \sin\theta_{n_{\bar{t}}} \sin\Delta\phi(n_t, n_{\bar{t}}), \qquad (28)$$

where $M_{t\bar{t}}$ is the invariant mass of the $t\bar{t}$ pair, the angles θ_{n_t} and $\theta_{n_{\bar{t}}}$ denote the polar angles of $\vec{n}_t$ and $\vec{n}_{\bar{t}}$ respectively and finally $\Delta\phi(n_t, n_{\bar{t}})$ is the angular difference between the projections of $\vec{n}_t$ and $\vec{n}_{\bar{t}}$ onto the plane perpendicular to $\vec{\bar{t}}$. If we define this angle within the range $[-\pi, \pi]$, we see from Eq. (28) that its sign will determine the sign of the TP. In this sense, the distribution of the number of the events with respect to the angle $\Delta\phi(n_t, n_{\bar{t}})$ is related to the asymmetry of the TP,

$$\mathcal{A}(\epsilon) = 1 - 2\frac{N(\epsilon < 0)}{N_T} \quad \text{and} \quad \frac{N(\epsilon < 0)}{N_T} = \int_{-\pi}^{0} \frac{1}{N_T} \frac{dN}{d\Delta\phi(n_t, n_{\bar{t}})} d\Delta\phi(n_t, n_{\bar{t}}), \qquad (29)$$

where N_T is the total number of events. Moreover, from a certain TP one can derive different angular distributions by considering different reference frames, but all of these will satisfy Eq. (29). In particular, we will analyze the following angular distributions based on the TPs defined in Sec. II:

- Related to $\epsilon_1 = \epsilon(t, \bar{t}, n_t, n_{\bar{t}})$ we consider $d\sigma/d\Delta\phi_1(n_t, n_{\bar{t}})$ in the rest frame of $t\bar{t}$ with $\vec{\bar{t}}$ in the z-axis. The angle $\Delta\phi_1(n_t, n_{\bar{t}})$ is the angular difference between the projection of the spin vectors in the plane perpendicular to $\vec{\bar{t}}$.

- Related to $\epsilon_2 = \epsilon(Q, \bar{t}, n_t, n_{\bar{t}})$ we consider $d\sigma/d\Delta\phi_2(n_t, n_{\bar{t}})$ in the rest frame of Q with $\vec{\bar{t}}$ in the z-axis. The angle $\Delta\phi_2(n_t, n_{\bar{t}})$ is the angular difference between the projection of the spin vectors in the plane perpendicular to $\vec{\bar{t}}$.

- Related to $\epsilon_3 = \epsilon(Q, t, n_t, n_{\bar{t}})$ we consider $d\sigma/d\Delta\phi_3(n_t, n_{\bar{t}})$ in the rest frame of Q with $\vec{t}$ in the z-axis. The angle $\Delta\phi_3(n_t, n_{\bar{t}})$ is the angular difference between the projection of the spin vectors in the plane perpendicular to $\vec{t}$.

In Fig. 5 we present the normalized distributions obtained for the first case listed above with $\kappa_t = 1, \tilde{\kappa}_t = 0$ (CP-even Higgs boson), $\kappa_t = 1, \tilde{\kappa}_t = \pm 1$ (CP-mixed Higgs boson) and $\kappa_t = 0, \tilde{\kappa}_t = 1$ (CP-odd Higgs boson). In Fig. 6 we display in turn the analogous distributions for ϵ_2. The distributions correponding to ϵ_3 are similar to those of ϵ_2 but with the opposite shift for $\kappa_t = \tilde{\kappa}_t = 1$ and $\kappa_t = -\tilde{\kappa}_t = 1$ and then we do not include them here.

FIG. 5: Angular distributions associated with the TP $\epsilon(t, \bar{t}, n_t, n_{\bar{t}})$ for various values of $(\kappa_t, \tilde{\kappa}_t)$. The error bars correspond to the statistical uncertainties.
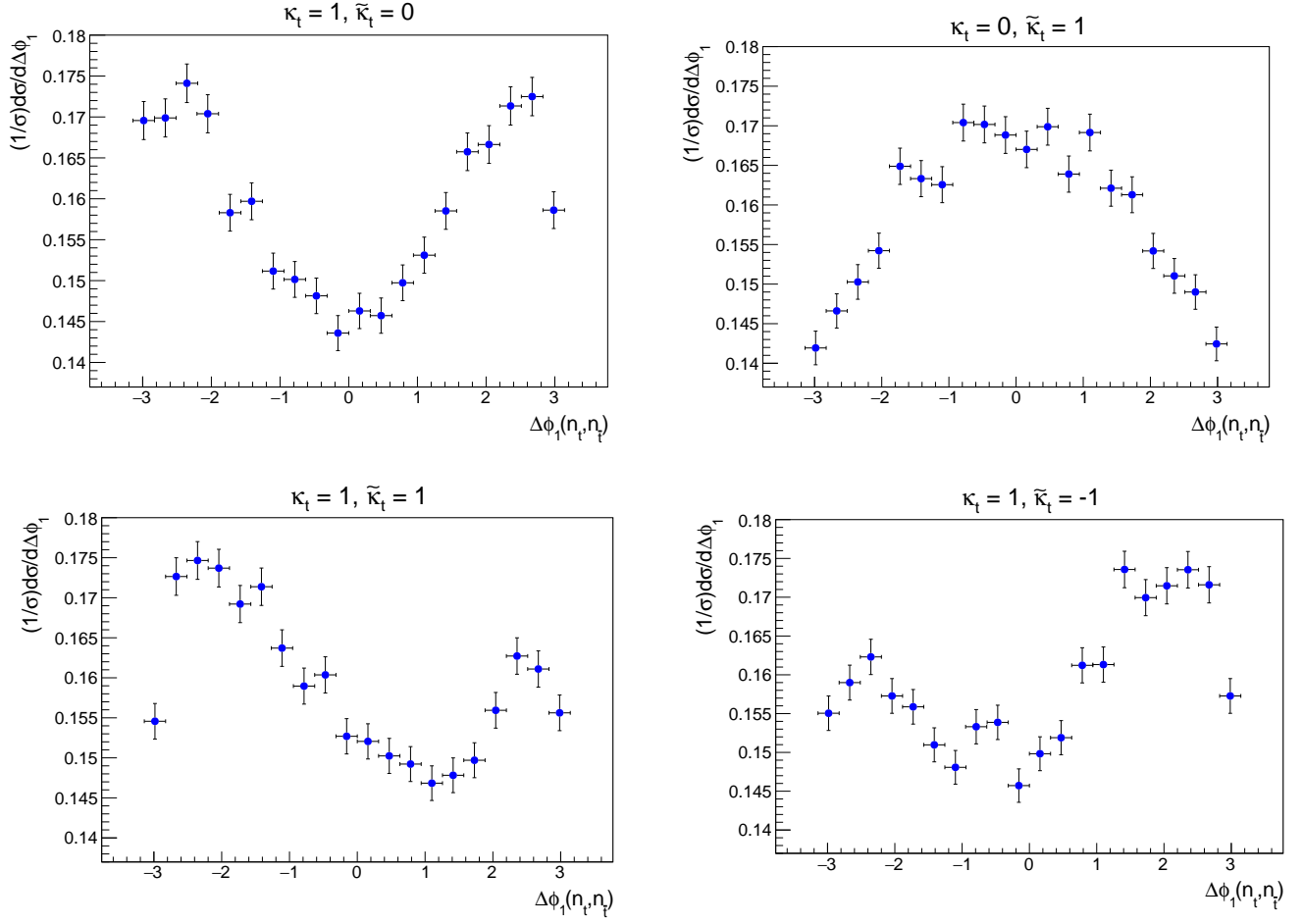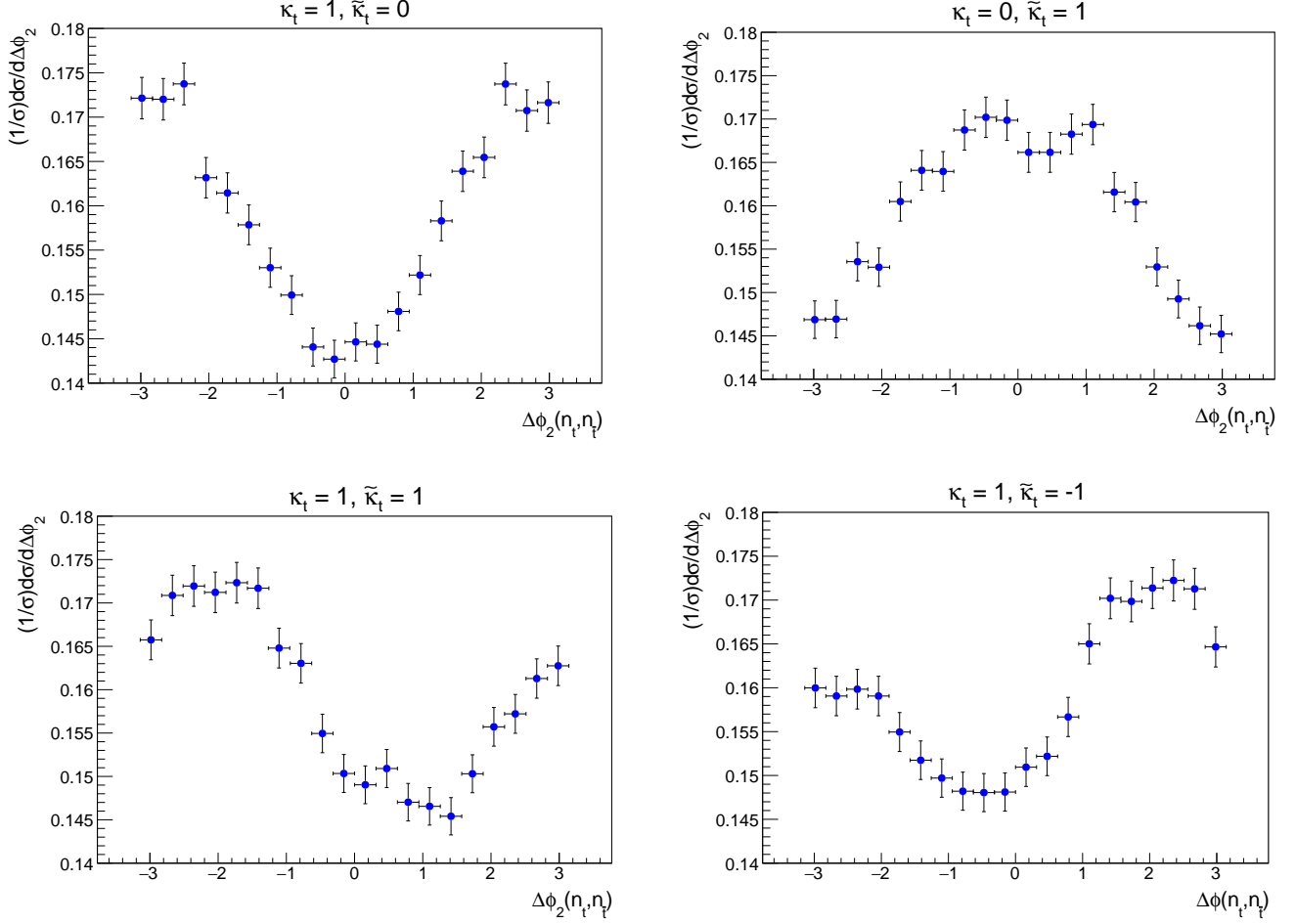
FIG. 6: Angular distributions associated with the TP $\epsilon(Q, \bar{t}, n_t, n_{\bar{t}})$ for various values of $(\kappa_t, \tilde{\kappa}_t)$. The error bars correspond to the statistical uncertainties.

As can be seen from Figs. 5 and 6, the peak of the distributions is shifted according to the values of the couplings $\kappa_t, \tilde{\kappa}_t$. This shift appears to be approximately the same but with opposite sign for $\kappa_t = \tilde{\kappa}_t = 1$ and $\kappa_t = -\tilde{\kappa}_t = 1$, distinguishing then the sign of the pseudoscalar coupling. The last is the expected behaviour since the asymmetry is linear in $\tilde{\kappa}_t$ (see Sec. III A) and the quantity $N(\epsilon < 0)/N_T$ is related to the angular distribution according to Eq. (29). The distributions for the SM and the pure pseudoscalar hypotheses are clearly different. While in the former case the distributions exhibit a minimum at $\Delta\phi_{1,2}(n_t, n_{\bar{t}}) = 0$, in the latter the similar distributions display a peak, so that the two hypotheses can be discriminated, in contrast to the asymmetry that vanishes for both hypotheses. In order to quantify the mentioned shifts, we have fitted the simulated distributions with the following function proposed in [14],

$$\frac{1}{\sigma}\frac{d\sigma}{d\Delta\phi_i(n_t, n_{\bar{t}})} = a_0 + a_1 \cos(\Delta\phi_i(n_t, n_{\bar{t}}) + \delta), \qquad i = 1, 2, 3. \tag{30}$$

To the extent that this equation is exact we note that Eq. (32) gives $\mathcal{A}(\epsilon_i) = 4a_1 \sin\delta$. With this fitting function, we obtain phase shifts approximately between 0.9 and 1 (-1 and -0.9)

14

for $\kappa_t = \tilde{\kappa}_t = 1$ ($\kappa_t = -\tilde{\kappa}_t = 1$) both for ϵ_1 and ϵ_2. However, the quality of the fits is not good enough, being worse in the case of the ϵ_1 distributions for which $\chi^2/\text{d.o.f}$ is in the range 1.69-3.86, in contrast to the range 0.53-1.16 obtained for ϵ_2. The main impact on the deviation from the functional form proposed in Eq. (30) appears to be caused by the ΔR_{ll} cut we have imposed. In fact, when this cut is turned off the above ranges for $\chi^2/\text{d.o.f}$ modify to 0.75-1.14 and 0.44-1.07 for the ϵ_1 and ϵ_2 distributions respectively. In Tables III and IV we list the results of the fits obtained when the $\Delta R_{\ell\ell}$ cut is relaxed. The results for the TP ϵ_3 are pretty similar to those for ϵ_2 but with opposite sign in the phase shifts of the CP-mixed hypotheses and hence we do not include them here. In addition, we show in Fig. 7 the angular distributions along with the fit curves for both CP-mixed cases when no cut is imposed in $\Delta R_{\ell\ell}$.

TABLE III: Fit results for the angular distribution $d\sigma/(\sigma d\Delta\phi_1(n_t, n_{\bar{t}}))$ related to the TP $\epsilon_1 = \epsilon(t, \bar{t}, n_t, n_{\bar{t}})$ when the $\Delta R_{\ell\ell}$ is turned off. Note that the parameter a_1 change its sign for $\kappa_t = 0, \kappa_t = 1$.

κ_t	$\tilde{\kappa}_t$	a_0	a_1	δ
1	−1	0.1592 ± 0.0006	-0.0139 ± 0.0008	0.81 ± 0.07
1	0	0.1595 ± 0.0006	-0.0181 ± 0.0008	0.002 ± 0.06
1	1	0.1591 ± 0.0006	-0.0131 ± 0.0008	-0.82 ± 0.07
0	1	0.1591 ± 0.0006	0.0102 ± 0.0008	0.11 ± 0.08

TABLE IV: Fit results for the angular distribution $d\sigma/(\sigma d\Delta\phi_2(n_t, n_{\bar{t}}))$ related to the TP $\epsilon_2 = \epsilon(Q, \bar{t}, n_t, n_{\bar{t}})$ when the $\Delta R_{\ell\ell}$ is turned off. Note that the parameter a_1 change its sign for $\kappa_t = 0, \kappa_t = 1$.

κ_t	$\tilde{\kappa}_t$	a_0	a_1	δ
1	−1	0.1591 ± 0.0006	-0.0146 ± 0.0008	0.73 ± 0.06
1	0	0.1594 ± 0.0007	-0.0190 ± 0.0008	0.005 ± 0.06
1	1	0.1592 ± 0.0006	-0.0136 ± 0.0008	-0.77 ± 0.07
0	1	0.1591 ± 0.0006	0.0113 ± 0.0008	0.09 ± 0.08

From Tables III and IV we see that the parameter δ is sensitive not only to the modulus of $\tilde{\kappa}_t$ but also to its sign, as expected if Eq. (29) is taken into account. The phase shift δ for the distribution of the angle $\Delta\phi_1$ appears to exhibit a slightly higher sensitivity than that obtained from the $\Delta\phi_2$-distribution, albeit both are still compatible within the statistical uncertainties. However, it is important to stress that the fits of the $\Delta\phi_2$-distributions give allways smaller values for $\chi^2/\text{d.o.f.}$
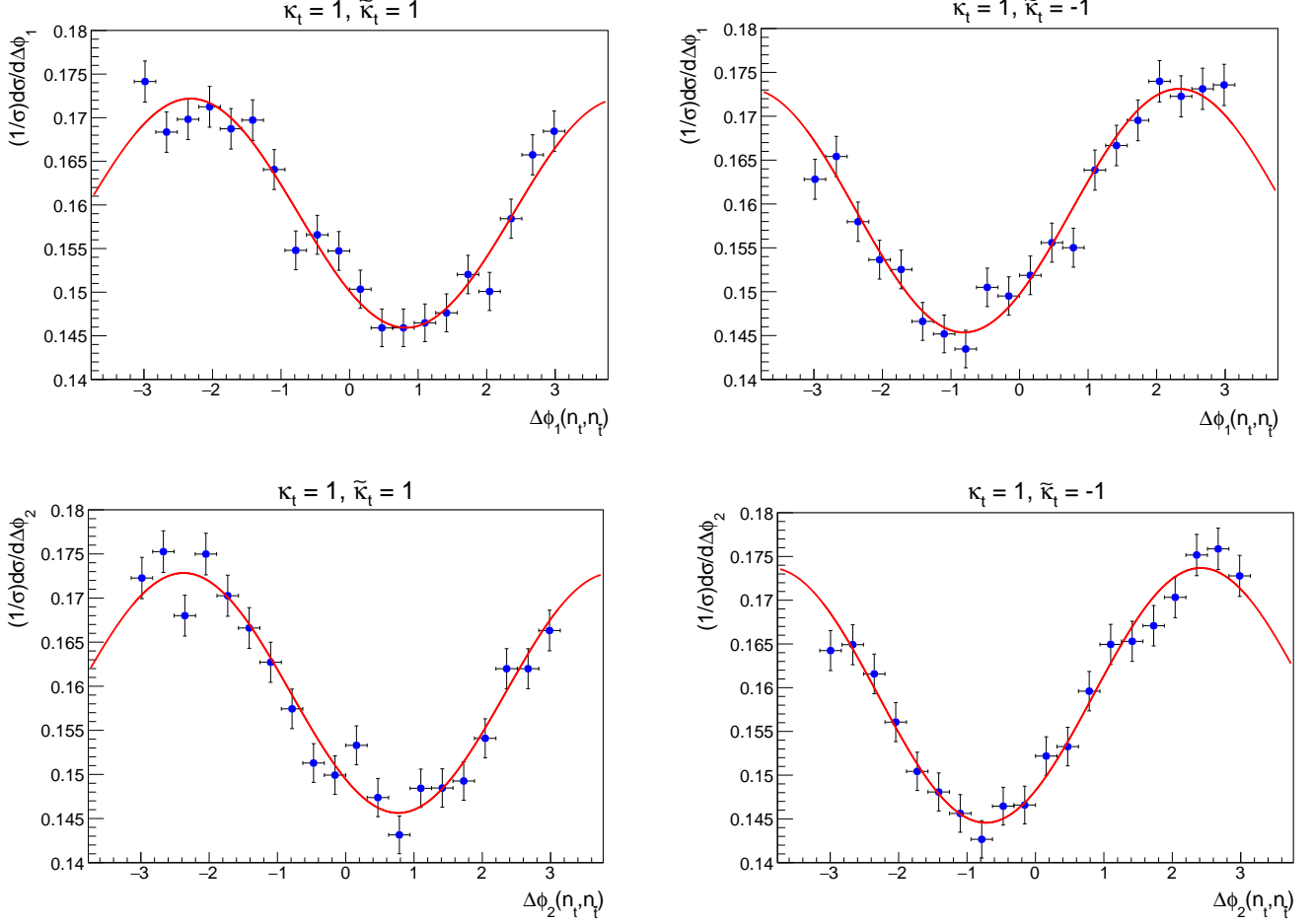
FIG. 7: Angular distributions $d\sigma/(\sigma d\Delta\phi_1(n_t, n_{\bar{t}}))$ (top) and $d\sigma/(\sigma d\Delta\phi_2(n_t, n_{\bar{t}}))$ (bottom) associated with the TPs $\epsilon_1 = \epsilon(t, \bar{t}, n_t, n_{\bar{t}})$ and $\epsilon_2 = \epsilon(Q, \bar{t}, n_t, n_{\bar{t}})$ respectively for the CP-mixed cases $\kappa_t = \tilde{\kappa}_t = 1$ (left) and $\kappa_t = -\tilde{\kappa}_t = 1$ (right) when the $\Delta R_{\ell\ell}$ cut is turned off. Also, the corresponding fit curves are displayed in red.

Concerning the angular distributions that can be related to the combination ϵ_4, we have analized the $\Delta\phi(n_t, n_{\bar{t}})$ distribution in the Q rest frame with H in the z-axis for various values of κ_t and $\tilde{\kappa}_t$. We have found that these distributions are not described by Eq. (30) and their range of variation is larger than that of the distributions displayed in Figs. 5 and 6. Unlike the distributions related to ϵ_1-ϵ_3, those arising from ϵ_4 exhibit small changes in their shapes for all the considered hypotheses and for this reason we have not included the corresponding plots here. However, the larger range of variation of the ϵ_4 distributions leads to higher values for the asymmetry (as can be sees from Tables I and II) even when the changes in the respective shapes are smaller than in the case of the distributions described by Eq. (30).

C. Mean value

We turn now to consider the last type of observables constructed from the TPs that are sensitive to $\tilde{\kappa}_t$, the mean value. Given a certain TP, we define its mean value in the following manner,

$$\langle \epsilon \rangle = \frac{\int \epsilon \left\{ d\sigma(pp \to b\,\ell^+ \nu_\ell \bar{b}\,\ell^- \bar{\nu}_\ell H)/d\Phi \right\} d\Phi}{\int \left\{ d\sigma(pp \to b\,\ell^+ \nu_\ell \bar{b}\,\ell^- \bar{\nu}_\ell H)/d\Phi \right\} d\Phi}, \tag{31}$$

where Φ is the Lorentz invariant phase space corresponding to the final state $b\,\ell^+ \nu_\ell \bar{b}\,\ell^- \bar{\nu}_\ell H$. From Eq. (20) we see that only the terms linear in κ_t and $\tilde{\kappa}_t$ will contribute to the mean value, so that we expect this observable to be sensitive not only to the value but also to the relative sign of the couplings.

The results obtained for the TPs $\epsilon_1 = \epsilon(t, \bar{t}, n_t, n_{\bar{t}})$, $\epsilon_2 = \epsilon(Q, \bar{t}, n_t, n_{\bar{t}})$ and $\epsilon_3 = \epsilon(Q, t, n_t, n_{\bar{t}})$ introduced in Sec. II are displayed in Table V, where we list the deviation of the mean values from the SM case ($\tilde{\kappa}_t = 0$) in terms of the corresponding statistical uncertainty of the estimator of $\langle \epsilon \rangle$, $\bar{\epsilon}$.

TABLE V: Mean values obtained for the TPs $\epsilon_{1,2,3}$ for the SM case and two CP-mixed cases with opposite sign in the pseudoscalar coupling. The values are obtained by using 10^5 simulated events.

κ_t	$\tilde{\kappa}_t$	$\langle \epsilon_1 \rangle / \sigma_{\bar{\epsilon}_1}$	$\langle \epsilon_2 \rangle / \sigma_{\bar{\epsilon}_2}$	$\langle \epsilon_3 \rangle / \sigma_{\bar{\epsilon}_3}$
1	-1	4.26	4.94	-5.81
1	0	-0.91	-0.22	1.25
1	1	-7.98	-8.83	8.75

We see that the three observables are capable of disinguishing the SM case from both CP-mixed cases. Further, the observables are sensitive to the sign of $\tilde{\kappa}_t$ and the two CP-mixed cases are also clearly disentangled. The observables $\langle \epsilon_2 \rangle$ and $\langle \epsilon_3 \rangle$ appear to be slightly more sensitive than $\langle \epsilon_1 \rangle$. On the other hand, the mean value for the combination ϵ_4 introduced in Sec. III A gives slightly smaller values than those listed in Table V, with $-4.32, 1.11$ and 7.23 for the cases ($\kappa_t = 1, \tilde{\kappa}_t = -1, 0, 1$) respectively. As with the asymmetry, the hypotheses CP-even and CP-odd cannot be distinguished by the mean value that is also linear in both κ_t and $\tilde{\kappa}_t$ (see Eqs. (20) and (31)). By taking into account the results given in Sec. III A, we can conclude that the sensitivity to the NP contribution is smaller for the mean values than for the asymmetries of the TPs under consideration.

IV. CP-ODD OBSERVABLES NOT DEPENDING ON t AND $\bar{t}$ SPIN VECTORS

So far we have considered three TPs involving the momenta $t, \bar{t}$ and Q and the spin vectors n_t and $n_{\bar{t}}$ given in Eqs. (3)-(4). In fact, we have described the general form of the differential cross-section in terms of these vectors in Eq. (20). Here, we will take into account another possibilities

for the choice of the vectors from which the CP-odd observables can be constructed. From the definitions in Eqs. (3)-(4), we see that the TPs $\epsilon_{1,2,3}$ can be written as follows,

$$\epsilon(t,\bar{t},n_t,n_{\bar{t}}) = \frac{m_t^2}{(t\cdot\ell^+)(\bar{t}\cdot\ell^-)}\,\epsilon(t,\bar{t},\ell^-,\ell^+), \tag{32}$$

$$\epsilon(Q,\bar{t},n_t,n_{\bar{t}}) = \frac{m_t^2}{(t\cdot\ell^+)(\bar{t}\cdot\ell^-)}\left(\epsilon(t,\bar{t},\ell^-,\ell^+) + \epsilon(H,\bar{t},\ell^-,\ell^+) + \frac{(t\cdot\ell^+)}{m_t^2}\epsilon(H,\bar{t},t,\ell^-)\right) \tag{33}$$

$$\epsilon(Q,t,n_t,n_{\bar{t}}) = \frac{m_t^2}{(t\cdot\ell^+)(\bar{t}\cdot\ell^-)}\left(-\epsilon(t,\bar{t},\ell^-,\ell^+) + \epsilon(H,t,\ell^-,\ell^+) + \frac{(\bar{t}\cdot\ell^-)}{m_t^2}\epsilon(H,\bar{t},t,\ell^+)\right). \tag{34}$$

The above equations express the TPs studied in the last sections as linear combination of TPs involving the momenta $t,\bar{t},H,\ell^+$ and ℓ^-, with coefficients that are functions of phase space variables. These five momenta give rise to five TPs whose sensitivity can also be tested by means of the observables introduced in Secs. III A-III C. In the first place, we have found that TPs not including both lepton and anti-lepton momenta present a negligible sensitivity, and then we will concentrate here on the results obtained for the remaining TPs, $\epsilon_5 \equiv \epsilon(t,\bar{t},\ell^-,\ell^+), \epsilon_6 \equiv \epsilon(H,t,\ell^-,\ell^+)$ and $\epsilon_7 \equiv \epsilon(H,\bar{t},\ell^-,\ell^+)$. The Tables VI and VII summarize the results for these TPs.

TABLE VI: Mean values obtained for the TPs $\epsilon_{5,6,7}$ for the SM case and two CP-mixed cases with opposite sign in the pseudoscalar coupling. The values correspond to 10^5 simulated events.

κ_t	$\tilde{\kappa}_t$	$\langle\epsilon_5\rangle/\sigma_{\bar{\epsilon}_5}$	$\langle\epsilon_6\rangle/\sigma_{\bar{\epsilon}_6}$	$\langle\epsilon_7\rangle/\sigma_{\bar{\epsilon}_7}$
1	−1	3.98	−1.96	1.69
1	0	−0.43	1.25	0.74
1	1	−6.76	3.46	−3.29

TABLE VII: Asymmetries for the TPs $\epsilon_{5,6,7}$ for the SM case and the two CP-mixed cases defined by $\kappa_t = 1, \tilde{\kappa}_t = \pm 1$. The values correspond to 10^5 simulated events.

κ_t	$\tilde{\kappa}_t$	$\mathcal{A}(\epsilon_5)$	$\mathcal{A}(\epsilon_5)/\sigma_\mathcal{A}$	$\mathcal{A}(\epsilon_6)$	$\mathcal{A}(\epsilon_6)/\sigma_\mathcal{A}$	$\mathcal{A}(\epsilon_7)$	$\mathcal{A}(\epsilon_7)/\sigma_\mathcal{A}$
1	−1	0.0315	10.0	−0.0134	−4.2	0.0111	3.5
1	0	−0.0021	−0.7	−0.0011	−0.3	0.0009	0.3
1	1	−0.0379	−12.0	0.0143	4.5	−0.0137	−4.3

We see that the TP ϵ_5 gives rise to asymmetries and mean values that are clearly higher than those obtained from ϵ_6 and ϵ_7. This is in contrast to the TPs $\epsilon_{1,2,3}$, for which the asymmetries and mean values are comparable (see Tables I and V). We also note that the asymmetry for ϵ_5 is exactly the same as for ϵ_1 as was expected from Eq. (32) since the proportionality factor relating them is positive definite. Regarding the mean values, we see by comparing Tables V and VI that the TPs $\epsilon_{1,2,3}$ appear to have a higher sensitivity to the pseudoscalar coupling than $\epsilon_{5,6,7}$.

It is important to mention that in the $t\bar{t}$ rest frame the sign of the TP ϵ_5 is defined through the angle $\Delta\phi_{\ell^-\ell^+}$ (recall the discussion on Eq. (31)), which is the angular difference between the projections of the leptons momenta onto the plane perpendicular to $\vec{\bar{t}}$. By a similar argument to that discussed at the beginning of Sec. III B, we can construct an associated angular distribution that, being constrained by the $\mathcal{A}(\epsilon_5)$, will be also sensitive to the sign of the pseudoscalar coupling. This angular variable is nothing but that proposed in [14] as a useful CP-odd observable. Moreover, it is shown in [14] that this angular distribution follows the functional form given in Eq. (30). Due to the fact that this distribution is constrained by $\mathcal{A}(\epsilon_5)$ which is equal to $\mathcal{A}(\epsilon_1)$ and smaller than $\mathcal{A}(\epsilon_{2,3})$, the corresponding shifts (δ) obtained for different values of $\tilde{\kappa}_t$ are expected to be of the same order than those exhibited by the $\Delta\phi_1(n_t, n_{\bar{t}})$ distribution and somewhat smaller than those observed in the $\Delta\phi_2(n_t, n_{\bar{t}})$ distribution.

In analogy to the combination of TPs considered in Sec. III, we have found a combination of the TPs $\epsilon_{5,6,7}$ for which the asymmetry is enhanced with respect to ϵ_5-ϵ_7,

$$\epsilon_8 = 2\epsilon_5 - \epsilon_6 + \epsilon_7 = \epsilon(t + \bar{t} + H, t - \bar{t}, \ell^+, \ell^-). \tag{35}$$

We see from Eq. (35) that in the $t\bar{t}H$ rest frame $\epsilon_8 = M_{t\bar{t}H}(\vec{t} - \vec{\bar{t}}) \cdot (\vec{\ell^+} \times \vec{\ell^-})$, where $M_{t\bar{t}H}$ is the invariant mass of the system $t\bar{t}H$. Hence, in this reference frame the sign of the combination ϵ_8 is set by the quantity $(\vec{t} - \vec{\bar{t}}) \cdot (\vec{\ell^+} \times \vec{\ell^-})$. Taking into account Eqs. (27) and (35) along with the definition $Q = (t + \bar{t} + H)/2$, we see that the only relevant difference between ϵ_4 and ϵ_8 is that in the latter the spin vectors n_t and $n_{\bar{t}}$ have been replaced by the momenta of the leptons ℓ^+ and ℓ^- respectively. The values obtained for $\mathcal{A}(\epsilon_8)$ are shown in Table VIII. Compared to the TPs ϵ_5-ϵ_7 and ϵ_1, ϵ_3 (see Tables I and VII), the chosen combination exhibits a slightly higher sensitivity in the asymmetry for resolving the CP-mixed cases. This is not true in the case of the TPs ϵ_2 and ϵ_4, for which the asymmetry is larger (see Tables I, II and VIII). In particular, the comparison between ϵ_4 and ϵ_8 indicates that the use of the momenta of the leptons instead of the spin vectors produces a decrease in the sensitivity of the asymmetry.

From the TPs ϵ_5-ϵ_7 one can derive various angular distributions in the same manner we have discussed in Sec. III B for ϵ_1-ϵ_3. Of course, in this case the corresponding angle will be defined in terms of the momenta of the leptons instead of using the spin vectors. These distributions have the same behaviour than those derived from ϵ_1-ϵ_3, but only the shift obtained in the case of ϵ_5 is compatible to the values given in Tables for ϵ_1-ϵ_3. The shifts resulting from the fit of the distributions related to ϵ_6 and ϵ_7 are smaller. Taking into account these facts we do not give further details of the angular distributions for the TPs discussed in this section.

The mean value of ϵ_8 for the hypotheses under consideration is comparable with the values listed in Table VI for ϵ_5. Concerning the associated angular distributions, their range of variation is larger than in the case of the distributions related to ϵ_5-ϵ_7 but exhibit smaller changes in their shapes for the different hypothesis and for this reason we do not include here the corresponding plots.

TABLE VIII: Asymmetry for the TP ϵ_8 for the SM case and the two CP-mixed cases defined by $\kappa_t = 1, \tilde{\kappa}_t = \pm 1$. The values are obtained with 10^5 simulated events.

κ_t	$\tilde{\kappa}_t$	$\mathcal{A}(\epsilon_8)$	$\mathcal{A}(\epsilon_8)/\sigma_{\mathcal{A}}$
1	-1	0.0331	10.5
1	0	0.0023	0.7
1	1	-0.0403	-12.7

V.   CP-ODD OBSERVABLES NOT DEPENDING ON t AND $\bar{t}$ MOMENTA

All the observables discussed in the above sections involve the momenta of the top and anti-top quarks thus requiring the full reconstruction of the kinematics of the individual t and $\bar{t}$ systems in order to be measured. Although challenging due to the presence of two neutrinos in the final state, this can be in principle done by applying a kinematic reconstruction method such that the neutrino weighting technique [25, 26]. Another possibility is to define observables that are not dependent on the t and $\bar{t}$ momenta but make use of the quarks b and $\bar{b}$. In order to construct such observables we will modify here the most sensitive observables studied in Secs. III and IV, namely the combinations ϵ_4 and ϵ_8 respectively. Let us first consider the combination ϵ_8 defined in Eq. (35) and replace the top and antitop momenta by the bottom and antibottom momenta respectively. Thus, we define

$$\epsilon_9 = \epsilon(b + \bar{b} + H, b - \bar{b}, \ell^+, \ell^-). \tag{36}$$

Note that now the sign of the TP ϵ_9 is set by the sign of the quantity $(\vec{b} - \vec{\bar{b}}) \cdot (\vec{\ell^+} \times \vec{\ell^-})$ in the $b\bar{b}H$ rest frame. This quantity is in fact used in [10] but in the lab frame in order to define a CP-odd observable that only depends on lab frame variables. The values of the asymmetry for ϵ_9 are listed in Table IX. By comparing Tables VIII and IX we see that the use of the $b, \bar{b}$ instead of $t, \bar{t}$ leads to a decrese in the sensitivity of the asymmetry by $\sim 5\sigma$ for $\kappa_t = 1, \tilde{\kappa}_t = \pm 1$. However, the observable is still capable of discriminating not only between the two CP-mixed hypotheses but also between these and the SM case. We proceed now in a similar way with the combination ϵ_4. By using Eq. (27) along with the definitions of the spin vectors in Eqs. (3)-(4), we can write

$$\epsilon_4 = \frac{m_t^2}{(t \cdot \ell^+) \cdot (\bar{t} \cdot \ell^-)} \epsilon(Q, t - \bar{t}, \ell^-, \ell^+) + \frac{1}{(t \cdot \ell^+)} \epsilon(Q, t, \ell^+, \bar{t}) - \frac{1}{(\bar{t} \cdot \ell^-)} \epsilon(Q, \bar{t}, t, \ell^-). \tag{37}$$

Since the asymmetry is not changed by an overall positive definite factor, we will concentrate in the following combination arising from the expression in Eq. (37),

$$\epsilon(Q, t - \bar{t}, \ell^-, \ell^+) + \frac{(\bar{t} \cdot \ell^-)}{m_t^2} \epsilon(Q, t, \ell^+, \bar{t}) - \frac{(t \cdot \ell^+)}{m_t^2} \epsilon(Q, \bar{t}, t, \ell^-), \tag{38}$$

TABLE IX: Asymmetry for the TP ϵ_9 for the SM case and the two CP-mixed cases defined by $\kappa_t = 1, \tilde{\kappa}_t = \pm 1$. The values are obtained with 10^5 simulated events.

κ_t	$\tilde{\kappa}_t$	$\mathcal{A}(\epsilon_9)$	$\mathcal{A}(\epsilon_9)/\sigma_{\mathcal{A}}$
1	-1	0.0171	5.4
1	0	0.0010	0.3
1	1	-0.0247	-7.8

and instead of replacing t and $\bar{t}$ directly by b and $\bar{b}$, we use their visible parts, namely $b + \ell^+$ and $\bar{b} + \ell^-$ respectively. This results in the following definition

$$\epsilon_{10} = \epsilon(\tilde{Q}, c_{b\bar{b}}, \ell^-, \ell^+) - w_1\, \epsilon(\tilde{Q}, b, \bar{b}, \ell^+) + w_2\, \epsilon(\tilde{Q}, b, \bar{b}, \ell^-), \tag{39}$$

where $\tilde{Q} \equiv (b+\ell^++\bar{b}+\ell^-)/2$ stands for the visible part of Q, $c_{b\bar{b}} = (1-w_1)\, b - (1-w_2)\, \bar{b}$ and the weights $w_{1,2}$ are given by $(\bar{b}\cdot\ell^-)/m_t^2$ and $(b\cdot\ell^+)/m_t^2$ respectively. Also, the contribution m_ℓ^2/m_t^2 has been neglected both in w_1 and in w_2. Note that if we set $w_1 = w_2 = 0$, the combination ϵ_{10} reduces to $\epsilon_9/2$ and $\mathcal{A}(\epsilon_{10})$ becomes equal to $\mathcal{A}(\epsilon_9)$. The results obatined for the asymmetry of ϵ_{10} are given in Table X. By comparing Tables II and X we see again that the sensitivity of the asymmetry decreases when t and $\bar{t}$ are not included in the TP. Nevertheless, the combination ϵ_{10} remains a useful observable for discriminating the CP nature of the Higgs boson, with the corresponding asymmetry having a sensitivity even higher than that of ϵ_9, as can be checked by taking into account Tables IX and X. More precisely, the separation between the CP-mixed hypotheses is enhanced by about 3σ. This improvement in the asymmetry of ϵ_{10} with respect to ϵ_9 may be due to two facts. In the first place, as was pointed out in Sec. IV when comparing the TPs ϵ_4 and ϵ_8, the asymmetry appears to be higher when the spin vectors are used instead of the lepton momenta and we see from Eqs. (36) and (39) that ϵ_{10}, being obtained from ϵ_4, contains the information on the spin vectors, as opposed to ϵ_9 that depends directly on the lepton momenta because it is derived from ϵ_8. In the second place, in order to obtain ϵ_{10} we have replaced in the expression for ϵ_4 the top and antitop momenta by their visible part, while in the case of ϵ_9 the bottom and antibottom momenta have been used.

TABLE X: Asymmetry for the TP ϵ_{10} for the SM case and the two CP-mixed cases defined by $\kappa_t = 1, \tilde{\kappa}_t = \pm 1$. The values are obtained by using 10^5 simulated events.

κ_t	$\tilde{\kappa}_t$	$\mathcal{A}(\epsilon_{10})$	$\mathcal{A}(\epsilon_{10})/\sigma_{\mathcal{A}}$
1	-1	-0.0213	-6.7
1	0	0.0031	1.0
1	1	0.0300	9.5

By using our set of simulated events we have also tested, for comparison purposes, the asymmetry of the lab frame observable given in [10]. We have obtained that this observable appears to be slightly less sensitive than the combination ϵ_{10}, giving rise to a separation between the CP-mixed hypotheses smaller by about 1.4σ.

VI.   EXPERIMENTAL FEASIBILITY

By considering the mild selection cuts introduced in Sec. III, the SM cross section for $pp \rightarrow t\,(\rightarrow b\ell^+\nu_\ell)\,\bar{t}\,\left(\rightarrow \bar{b}\ell^-\bar{\nu}_\ell\right)\,H$, $\ell = e, \mu$ at $14\,\mathrm{TeV}$ is $\sim 15.3\,\mathrm{fb}$ and hence the number of events expected within the context of the HL-LHC is $\sim 15.3\,\mathrm{fb} \times 3000\,\mathrm{fb}^{-1} = 4.59 \times 10^4$. This number is expected to be even larger in the case of $\kappa_t = 1, \tilde{\kappa}_t \neq 0$ since the corresponding cross section is then higher than the SM one. By taking into account NLO corrections to the production process and considering a K-factor around 1.2 [27–29], the number of events can be raised up to $\sim 5.49 \times 10^4$. On the other hand, additional cuts as well as the efficiency related to the reconstruction of particles momenta will contribute to decrease this number. For instance, in order to obtain the asymmetry of ϵ_4, the t and $\bar{t}$ momenta need to be reconstructed. This is challenging not only due to the presence of two neutrinos in the final state which escape the detector undetected but also because final state objects need to be asocciated with the respective parent quark [25]. As was already mentioned in Sec. V, a possibility is to use the neutrino weighting technique along with the kinematic equations arising from kinematic constraints related to the top and W masses as well as from the energy-momentum conservation at each of the decay vertices involved in the process. Within the context of $t\bar{t}$ this procedure has been used, for instance, in order to obtain measurements of spin correlation [25] and charge asymmetry [26]. Also, events reconstructed with this technique has been used in [30] for analyzing angular distributions that are useful for discriminating the signal from the backgrounds in $t\bar{t}H(H \rightarrow b\bar{b})$. In all these cases the corresponding efficiency in the reconstruction of the momenta is up to $\sim 80\%$.

Based on the discussion given in the previous paragraph, we have simulated sets of $5\times10^4, 1\times 10^4$ and 5×10^3 events and recalculated the most sensitive observable, namely $\mathcal{A}(\epsilon_4)$, for each case. The results are displayed in Table XI, where it can be seen that for a number of events close to that roughly estimated above within the context of the HL-LHC, the observable is still sensitive to $\tilde{\kappa}_t$ allowing to separate the CP-mixed cases by 19σ. As expected, the sensitivity worsen as the number of events is reduced, but even with 5×10^3 events the separation between the CP-mixed hypotheses under consideration is around 6.5σ.

Although the combination ϵ_{10} discussed in Sec. V avoids the problem of reconstructing the top and antitop momenta, we have also considered the respective asymmetry obtained for more conservative numbers of events. In Table XII we show the results for $\mathcal{A}(\epsilon_{10})$ when the number of events is reduced from 5×10^4 to 1×10^4. We see in this case that even with 1×10^4 simulated events the observable is capable to discriminate the CP-mixed cases by 5.6σ.

Finally, it is important to mention that a realistic analysis of the sensitivity of the observables discussed in this paper requires the study of the impact of the backgrounds as well as the hadronization of the quarks in the final state and the effects of the detector. If we consider the dominant decay mode of the higgs, $H \rightarrow b\bar{b}$, in order to maximize the cross section of the process, the signature is given by 4 b-jets, two leptons and missing energy, while the main background arise from the production of $t\bar{t}$ in asocciation with additional jets, being the dominant source the production of $t\bar{t} + b\bar{b}$. By applying a small set of cuts it is shown in [31] that the

TABLE XI: Asymmetry for the TP ϵ_4 obtained by using $5 \times 10^4, 1 \times 10^4$ and 5×10^3 simulated events for the SM case and the two CP-mixed cases defined by $\kappa_t = 1, \tilde{\kappa}_t = \pm 1$.

κ_t	$\tilde{\kappa}_t$	$N_{\text{ev}} = 5 \times 10^4$		$N_{\text{ev}} = 1 \times 10^4$		$N_{\text{ev}} = 5 \times 10^3$	
		$\mathcal{A}(\epsilon_4)$	$\mathcal{A}(\epsilon_4)/\sigma_{\mathcal{A}}$	$\mathcal{A}(\epsilon_4)$	$\mathcal{A}(\epsilon_4)/\sigma_{\mathcal{A}}$	$\mathcal{A}(\epsilon_4)$	$\mathcal{A}(\epsilon_4)/\sigma_{\mathcal{A}}$
1	-1	-0.0405	-9.1	-0.0426	-4.3	-0.0496	-3.5
1	0	0.0004	0.1	-0.0084	-0.8	-0.0004	-0.03
1	1	0.0443	9.9	0.0434	4.2	0.0420	3.0

TABLE XII: Asymmetry for the TP ϵ_{10} in the SM case and the two CP-mixed cases defined by $\kappa_t = 1, \tilde{\kappa}_t = \pm 1$ when the number of simulated events is reduced from 5×10^4 to 1×10^4.

κ_t	$\tilde{\kappa}_t$	$N_{\text{ev}} = 5 \times 10^4$		$N_{\text{ev}} = 1 \times 10^4$	
		$\mathcal{A}(\epsilon_{10})$	$\mathcal{A}(\epsilon_{10})/\sigma_{\mathcal{A}}$	$\mathcal{A}(\epsilon_{10})$	$\mathcal{A}(\epsilon_{10})/\sigma_{\mathcal{A}}$
1	-1	-0.0270	-6.0	-0.0184	-1.8
1	0	0.0022	0.5	-0.0086	-0.9
1	1	0.0313	7.0	0.0380	3.8

signal to background ratio is largely improved. On the other hand, a rigorous treatment of the backgrounds and their impact with respect to the signal is performed in [32] by using $20.3 \, \text{fb}^{-1}$ of data at $\sqrt{s} = 8 \, \text{TeV}$.

The results shown in tables XI and XII reveal that with 5×10^3 and 1×10^4 events respectively the observables $\mathcal{A}(\epsilon_4)$ and $\mathcal{A}(\epsilon_{10})$ are still useful for testing $\tilde{\kappa}_t$. Without considering the lack of events related to the experimental analysis, these numbers of events correspond to a luminosity around ~ 300 - $600 \, \text{fb}^{-1}$ for the SM and even smaller for the CP-mixed cases due to the larger cross section. This range of luminosities is in principle achievable in the short term by the LHC. We note that in order to be fully conclusive about the required luminosity, it is important to include the effects of hadronization, detector resolution, reconstruction eficciencies and so forth. However, this kind of analysis is out of the scope of this paper.

VII. CONCLUSIONS

In this paper we have presented a collection of CP-odd observables based on triple product correlations that are useful for disentangling the relative sign between the scalar (κ_t) and a potential pseudoscalar ($\tilde{\kappa}_t$) top-Higgs couplings in the $t\bar{t}H$ production with both tops decaying

leptonically. We have tested the sensitivity of the proposed observables by considering three types of observables: asymmetries, mean values and angular distributions.

Through the use of spinor techniques we have written the expression for the differential cross section of the full process in such a manner that the production and the decay parts are separated, although connected by the spin vectors of the top and antitop which are given in terms of the momenta of the leptons in the final state. Moreover, we have indentified the terms linear in κ_t and $\tilde{\kappa}_t$ as those involving TPs. Among these, we have explored the three that do not involve the momenta of the incoming quarks/gluons and at the same time incorporate both spin vectors: $\epsilon_1 \equiv \epsilon(t, \bar{t}, n_t, n_{\bar{t}})$, $\epsilon_2 \equiv \epsilon(Q, \bar{t}, n_t, n_{\bar{t}})$ and $\epsilon_3 \equiv \epsilon(Q, t, n_t, n_{\bar{t}})$.

We have found that $\epsilon_{1,2,3}$ allow to distinguish between the CP-mixed hypotheses by more than $\sim 20\sigma$ in the case of asymmetries and $\sim 10\sigma$ in the case of mean values when 1×10^5 simulated events are used. Furthermore, we have shown that the angular distributions asocciated with these TPs are also sensitive to the value of κ_t and $\tilde{\kappa}_t$ exhibiting a phase shift that varies according to the values taken by these couplings. On the other hand, by exploring TPs that incorporate the momenta of the Higgs and the leptons instead of the spin vectors we can conclude that the observables studied here appear to be more sensitive when the spin vectors are used.

On the other hand, we have proposed a combination of the TPs considered in the first place, $\epsilon_4 \equiv \epsilon_3 - \epsilon_2$, that exhibits the highest sensitivity with the separation between the CP-mixed hypotheses being increased by at least 3σ in the asymmetry for 1×10^5 events with respect to $\mathcal{A}(\epsilon_{1,2,3})$. Again, when a similar combination is constructed by using the leptons momenta instead of the spin vectors (ϵ_8), the sensitivity in the asymmetry is decreased by $\sim 3\sigma$ compared to $\mathcal{A}(\epsilon_4)$ for the same number of events, giving values compatible with those obtained for the asymmetry of ϵ_2 and ϵ_3.

Taking into account the challenge of reconstructing the top and antitop momenta due to the presence of two neutrinos in the final state, we have proposed and tested two TP correlations that avoid this difficulty. The first one is obtained by replacing the t and $\bar{t}$ by the b and $\bar{b}$ momenta (ϵ_9), whereas the second includes the visible part of the t and $\bar{t}$ momenta (ϵ_{10}). We have encountered that the latter is the most sensitive leading to a discrimination of the CP-mixed cases under analysis by up to $\sim 16\sigma$.

Finally we have discussed the feasibility of the most sensitive observables proposed here. We have found that with 5×10^3 and 1×10^4 events respectively the observables $\mathcal{A}(\epsilon_4)$ and $\mathcal{A}(\epsilon_{10})$ are still useful for testing the hypotheses ($\kappa_t = 1, \tilde{\kappa}_t = \pm 1$) giving rise to separations of order $\sim 6\sigma$. These required number of events would be reachable in principle in the short term by the LHC and hence the capability of the observables studied here for testing the sign of $\tilde{\kappa}_t/\kappa_t$ could be probed in that context.

REFERENCES

[1] G. Aad *et al.*, Physics Letters B **716**, 1 (2012).

[2] S. Chatrchyan *et al.*, Physics Letters B **716**, 30 (2012).

[3] J. Brod, U. Haisch, and J. Zupan, Journal of High Energy Physics **2013**, 180 (2013), 10.1007/JHEP11(2013)180.

[4] J. Ellis and T. You, Journal of High Energy Physics **2013**, 103 (2013), 10.1007/JHEP06(2013)103.

[5] A. Djouadi and G. Moreau, The European Physical Journal C **73**, 2512 (2013), 10.1140/epjc/s10052-013-2512-9.

[6] K. Cheung, J. Lee, and P.-Y. Tseng, Journal of High Energy Physics **2013**, 134 (2013), 10.1007/JHEP05(2013)134.

[7] J. Baron *et al.* (ACME Collaboration), Science **343**, 269 (2014).

[8] R. Harnik, A. Martin, T. Okui, R. Primulando, and F. Yu, Phys. Rev. D **88**, 076009 (2013).

[9] M. Farina, C. Grojean, F. Maltoni, E. Salvioni, and A. Thamm, Journal of High Energy Physics **2013**, 22 (2013), 10.1007/JHEP05(2013)022.

[10] F. Boudjema, D. Guadagnoli, R. M. Godbole, and K. A. Mohan, Phys. Rev. D **92**, 015019 (2015).

[11] J. F. Gunion and X.-G. He, Phys. Rev. Lett. **76**, 4468 (1996); J. F. Gunion, B. Grzadkowski, and X.-G. He, *ibid.* **77**, 5172 (1996); J. F. Gunion and J. Pliszka, Physics Letters B **444**, 136 (1998); X.-G. He, G.-N. Li, and Y.-J. Zheng, International Journal of Modern Physics A **30**, 1550156 (2015).

[12] G. Mahlon and S. Parke, Phys. Rev. D **53**, 4886 (1996); Physics Letters B **411**, 173 (1997); Phys. Rev. D **81**, 074024 (2010); D. Atwood, A. Aeppli, and A. Soni, Phys. Rev. Lett. **69**, 2754 (1992).

[13] S. Biswas, R. Frederix, E. Gabrielli, and B. Mele, Journal of High Energy Physics **2014**, 20 (2014), 10.1007/JHEP07(2014)020.

[14] J. Ellis, D. Hwang, K. Sakurai, and M. Takeuchi, Journal of High Energy Physics **2014**, 4 (2014), 10.1007/JHEP04(2014)004.

[15] O. Antipin and G. Valencia, Phys. Rev. D **79**, 013013 (2009); G. Valencia, *Proceedings on 11th International Conference on Heavy Quarks and Leptons (HQL 2012)*, PoS **HQL2012**, 050 (2012), arXiv:1301.0962 [hep-ph].

[16] A. Hayreter and G. Valencia, Phys. Rev. D **88**, 034033 (2013).

[17] T. Arens and L. M. Sehgal, Phys. Rev. D **50**, 4372 (1994).

[18] S. Kawasaki, T. Shirafuji, and S. Y. Tsai, Prog. Theor. Phys. **49**, 1656 (1973).

[19] P. Saha, K. Kiers, B. Bhattacharya, D. London, A. Szynkman, and J. Melendez, (2015), arXiv:1510.00204 [hep-ph]; P. Saha, K. Kiers, D. London, and A. Szynkman, Phys. Rev. **D90**, 094016 (2014), arXiv:1407.1725 [hep-ph]; K. Kiers, P. Saha, A. Szynkman, D. London, S. Judge, and J. Melendez, **D90**, 094015 (2014), arXiv:1407.1724 [hep-ph]; K. Kiers, T. Knighton, D. London, M. Russell, A. Szynkman, and K. Webster, **D84**, 074018 (2011), arXiv:1107.0754 [hep-ph].

[20] R. Kleiss and W. Stirling, Nuclear Physics B **262**, 235 (1985).

[21] M. L. Mangano and S. J. Parke, Physics Reports **200**, 301 (1991).

[22] H. W. Fearing and S. Scherer, Phys. Rev. D **53**, 315 (1996).

[23] W. Bernreuther, A. Brandenburg, Z. Si, and P. Uwer, Nuclear Physics B **690**, 81 (2004).

[24] J. Alwall, R. Frederix, S. Frixione, V. Hirschi, F. Maltoni, O. Mattelaer, H.-S. Shao, T. Stelzer, P. Torrielli, and M. Zaro, Journal of High Energy Physics **2014**, 79 (2014), 10.1007/JHEP07(2014)079.

[25] *Measurements of spin correlation in top-antitop quark events from proton-proton collisions at $s = 7$ TeV using the ATLAS detector*, Tech. Rep. ATLAS-CONF-2013-101 (CERN, Geneva, 2013).

[26] G. Aad *et al.*, Journal of High Energy Physics **2015**, 61 (2015), 10.1007/JHEP05(2015)061.

[27] S. Dawson, L. H. Orr, L. Reina, and D. Wackeroth, Phys. Rev. D **67**, 071503 (2003).

[28] W. Beenakker, S. Dittmaier, M. Kramer, B. Plumper, M. Spira, and P. Zerwas, Nuclear Physics B **653**, 151 (2003).

[29] S. Dittmaier *et al.* (LHC Higgs Cross Section Working Group), *Handbook of LHC Higgs Cross Sections: 1. Inclusive Observables* (CERN, Geneva, 2011).

[30] S. P. Amor dos Santos, J. P. Araque, R. Cantrill, N. F. Castro, M. C. N. Fiolhais, R. Frederix, R. Gonçalo, R. Martins, R. Santos, J. Silva, A. Onofre, H. Peixoto, and A. Reigoto, Phys. Rev. D **92**, 034021 (2015).

[31] H.-L. Li, P.-C. Lu, Z.-G. Si, and Y. Wang, (2015), arXiv:1508.06416 [hep-ph].

[32] G. Aad *et al.*, The European Physical Journal C **75**, 349 (2015), 10.1140/epjc/s10052-015-3543-1.